THE JOURNAL OF PHYSICAL CHEMISTRY B

Article

pubs.acs.org/JPCB

Characterizing Generated Charged Inverse Micelles with Transient Current Measurements

Filip Strubbe,* Manoj Prasad, and Filip Beunis

Electronics and Information Systems and Center for Nano and Biophotonics (NB-Photonics), Ghent University, Sint-Pietersnieuwstraat 41, Ghent B-9000, Belgium

Supporting Information

ABSTRACT: We investigate the generation of charged inverse micelles in nonpolar surfactant solutions relevant for applications such as electronic ink displays and liquid toners. When a voltage is applied across a thin layer of a nonpolar surfactant solution between planar electrodes, the generation of charged inverse micelles leads to a generation current. From current measurements it appears that such charged inverse micelles generated in the presence of an electric field behave differently compared to those present in equilibrium in the absence of a field. To examine the origin of this difference, transient current measurements in which the applied voltage is suddenly increased are used to measure the mobility and the amount of generated charged inverse micelles. The mobility and the corresponding hydrodynamic size are found to be similar to those of charged inverse micelles present in equilibrium, which indicates that other properties determine their different behavior. The amplitude and shape of the transient currents measured as a function of the surfactant concentration confirm that the charged inverse micelles are generated by bulk disproportionation. A theoretical model based on bulk disproportionation with simulations and analytical approximations is developed to analyze the experimental transient currents.

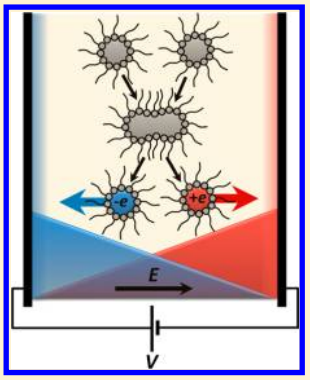

1. INTRODUCTION

Nonpolar liquids with added surfactant are studied intensively for their relevance in motor oil,[1,2] petroleum processing,[3] electrical power transformers,[4] electronic ink displays, and liquid toners.[5−7] In many applications surfactants are used as charging and stabilizing agents for colloidal particles. Since not all added surfactant resides on the particles or at other interfaces, the excess surfactant can form inverse micelles of which a small fraction is charged. These charged inverse micelles are the origin of the often surprisingly high electrical conductivity measured in nonpolar surfactant solutions.[8−14] This conductivity in turn affects the switching behavior if colloidal particles are present.[15−18] Measurements based on the pair interaction potential, particle tracking electrophoresis, optical trapping electrophoresis, and blinking tweezers are currently used to probe the electrokinetic properties of nonpolar colloids.[7,9−11,15−24] To isolate the effects of the charged inverse micelles, mixtures of pure nonpolar liquid with surfactant are often investigated without the presence of colloidal particles. Transient current measurements have provided insight in the complex dynamics of charges in nonpolar surfactant when electrical fields are applied.[25−35] In general, the electrical behavior of a nonpolar surfactant system is governed by generation of charged inverse micelles (and the inverse recombination process), by diffusion and drift in an electric field, and by the behavior of the micelles at the electrode interfaces. Measurements of many different nonpolar surfactant systems show that this electrical behavior roughly leads to two categories of nonpolar surfactant solutions. In the first category charged inverse micelles are generated much faster than they can be transported by typical electrical fields to the attracting electrodes. Then the bulk concentration of charged inverse micelles remains roughly equal to the equilibrium concentration. This is the case for surfactant systems with small inverse micelles such as AOT and SPAN85.[32,33] With these surfactants the charged inverse micelles that are attracted to the oppositely charged electrodes get adsorbed there and form thin charged interface layers. This leads to an overall electrical behavior that can be modeled as a resistor in series with interface capacitances. In the second category of nonpolar surfactant systems, which typically occurs for larger micelles such as Solsperse13940, SPAN80, and OLOA11K, generated charged inverse micelles are transported to the electrodes faster than they are generated at typical applied voltages. Then the equilibrium concentration of charges in the bulk is much lower than the equilibrium concentration.[27,31,34] In these surfactant systems, at applied voltages above 1 V, the initially present charged inverse micelles can be separated, leaving the bulk almost depleted of charge.[16,27−30] The charged inverse micelles which are attracted to the electrodes do not adsorb at the interfaces but instead form a diffuse double layer.[36] Therefore, the lower generation rate and different behavior at the electrodes lead to a different overall electrical behavior. The transient electrical current due to the separation of the initially present charged micelles can be observed clearly and can be used to obtain the concentration,

Received: November 13, 2014
Revised: January 9, 2015
Published: January 12, 2015

DOI: 10.1021/jp511378k
J. Phys. Chem. B 2015, 119, 1957−1965

mobility, and hydrodynamic size of the charged inverse micelles. The remaining nonzero current after the transient is related to and limited by the generation of new charged inverse micelles. This generation current can be used to investigate the mechanism and rate with which the charges are generated.[34]

In this paper a more detailed investigation of the charge generation process in a nonpolar surfactant system is carried out. We investigate the surfactant polyisobutylene succinimide (PIBS) commercially sold as OLOA11K in *n*-dodecane. This surfactant is an interesting model system since it has large, slow micelles and a low generation current, and it behaves similar to other surfactants such as Solsperse13940 and SPAN80. Even though many aspects of the generation mechanism of charged inverse micelles in this surfactant system are well-understood, measurements of reversal currents in which the voltage is switched from V to $-V$ have revealed a difference between charged inverse micelles present in equilibrium in the absence of an electric field and charged inverse micelles that are newly generated in the presence of a field (unpublished results). In these reversal currents a first maximum occurs which is understood well from drift and diffusion of the initially present charges, but also a second peak is observed that cannot be explained by the existing theoretical model. The second peak is related to newly generated charged inverse micelles since it is absent for short times of the preceding pulse at voltage V and since it grows (until saturation is reached) if the preceding pulse during which new charges are generated is longer. The fact that the second peak appears at a different time than the expected arrival time of the initially present charges could mean that it is caused by charges with a different mobility. Also, in contrast to the initially present charges, the newly generated charges practically do not contribute to the charge inside the double layer. Altogether, it is clear that newly generated charges behave differently at the electrode surfaces and potentially have a different mobility compared to the initially present charges. Such different behavior could originate from a difference in size or charge-distribution of the inverse micelles. Here, the number and the mobility of newly generated charged inverse micelles is measured using transient current measurements with stepwise increasing voltage ($V_1 \rightarrow V_2$). Such information cannot be achieved using just polarizing voltages (0 V$\rightarrow V$) since this provides only the generation rate of charged inverse micelles but not the mobility or the concentration separately.[34] At the same time the amplitude and shape of the measured currents confirm that the newly generated charges are formed by a bulk disproportionation mechanism.

2. THEORY

For the interpretation of transient currents with stepwise increasing voltages ($V_1 \rightarrow V_2$) a theoretical model with simulations and analytical formulas is developed in this section. In this model we consider a suspension of inverse micelles placed between two parallel electrodes. We assume that bulk disproportionation ($2A_0 \leftrightarrow A_- + A_+$) is the generation mechanism leading to charged inverse micelles. Then, in equilibrium and in absence of an electric field, the concentration of positively and negatively charged inverse micelles is $n_+ = n_- = \overline{n} = (\beta/\alpha)^{1/2}\overline{n}_0$.[10,11,34,36] Here, $\overline{n}$ and $\overline{n}_0$ are defined as the equilibrium concentrations of charged and uncharged inverse micelles respectively, and β and α are the generation and recombination rate constants of the disproportionation mechanism. Since the formation of a charged inverse micelle comes at a large free energy cost, we can restrict to the case that $\beta \ll \alpha$ and therefore that $\overline{n} \ll \overline{n}_0$.[10] When a voltage difference is applied across the electrodes, the transient current $I(t)$ can be modeled with[27,30]

$$I(t) = \sum_i z_i e S \frac{1}{d} \int_0^d \Psi_i \mathrm{d}x \tag{1}$$

Here, x is the position between the electrodes which are situated at $x = 0$ and $x = d$, e is the elementary charge, S is the surface area of the electrodes, and z_i is the valency of micelles where the index i refers to positive, negative, or neutral inverse micelles. The flux due to drift in the electric field E and due to diffusion is $\Psi_i = En_i\mu_i - D_i(\mathrm{d}n_i/\mathrm{d}x)$. We will make a distinction between positively and negatively charged micelles which are initially present in equilibrium in absence of an electric field, with concentrations respectively n_+ and n_- with a mobility $\mu_+ = -\mu_- = \mu$, valency $z_+ = -z_- = z$, and diffusion coefficient $D_+ = D_- = D$ and the newly generated positively and negatively charged inverse micelles with concentration respectively $n_{\mathrm{gen},+}$ and $n_{\mathrm{gen},-}$ with mobility $\mu_{\mathrm{gen},+} = -\mu_{\mathrm{gen},-} = \mu_{\mathrm{gen}}$, $z_{\mathrm{gen},+} = -z_{\mathrm{gen},-} = z_{\mathrm{gen}}$ and $D_{\mathrm{gen},+} = D_{\mathrm{gen},-} = D_{\mathrm{gen}}$. The diffusion coefficient and mobility are related by $D_i = \mu_i kT/ze$, with Boltzmann constant k and temperature T. Considering the small size of the micelles compared to the Bjerrum length in nonpolar liquids we expect a value $z = z_{\mathrm{gen}} = 1$ for both types of charged inverse micelles.[27,29] However, the size and therefore also the mobility and diffusion coefficient of the initially present and newly generated charged inverse micelles can potentially be different. The dynamics of the concentrations are determined by the following continuity equations and Gauss's law:

$$\frac{\mathrm{d}n_\pm}{\mathrm{d}t} = -\frac{\mathrm{d}\Psi_\pm}{\mathrm{d}x} \tag{2}$$

$$\frac{\mathrm{d}n_{\mathrm{gen},\pm}}{\mathrm{d}t} = -\frac{\mathrm{d}\Psi_{\mathrm{gen},\pm}}{\mathrm{d}x} + \beta n_0^2 - \alpha n_{\mathrm{tot},+} n_{\mathrm{tot},-} \tag{3}$$

$$\frac{\mathrm{d}n_0}{\mathrm{d}t} = -\frac{\mathrm{d}\Psi_0}{\mathrm{d}x} - 2(\beta n_0^2 - \alpha n_{\mathrm{tot},+} n_{\mathrm{tot},-}) \tag{4}$$

$$\varepsilon_0 \varepsilon_r \frac{\mathrm{d}E}{\mathrm{d}x} = \rho \tag{5}$$

Here, ε_0 is the permittivity of vacuum, ε_r is the dielectric constant of the liquid, t is time, and $\rho = \sum_i z_i e n_i$ is the space charge density conserving overall charge neutrality $\int_0^d \rho \, \mathrm{d}x = 0$. In the simulations, eqs 1−5 are solved numerically with boundary conditions $\int_0^d E \, \mathrm{d}x = V_j$ where V_j is the applied voltage with normalized value $\varphi_j = (zeV_j/kT)$. Blocking conditions for the inverse micelles are assumed at the electrodes: $\Psi_i(x = 0) = \Psi_i(x = d) = 0$. This is a simplification since we will see in the experiments that at high applied voltages there are additional, but small contributions to the current such as surface generation currents. In eq 2 we assume that the total number $\overline{n}dS$ of initially present positively and negatively charged inverse micelles is fixed, hence the absence of generation and recombination terms. In eqs 3 and 4 we assume that the newly generated inverse micelles can also recombine with initially present micelles. Therefore, the recombination term $\alpha n_{\mathrm{tot},+} n_{\mathrm{tot},-}$ scales with the concentrations $n_{\mathrm{tot},\pm} = n_\pm + n_{\mathrm{gen},\pm}$. The neutral inverse micelles with concentration n_0, with diffusion coefficient $D_0 = D$, but with zero charge and mobility do not contribute to the current.

DOI: 10.1021/jp511378k
J. Phys. Chem. B 2015, 119, 1957−1965

Next, analytical approximations are derived that offer insight in the measured and simulated transient currents. We restrict to the case of $\varphi_j \gg 1$ such that diffusion in the bulk can be ignored.[28] The bulk region is defined as the volume between the electrodes excluding the thin double layers with thickness approximately $2d/\varphi_j$.[27] Of course, inside the thin double layers at the electrodes diffusion still plays an important role. We also restrict to low generation rates and high electric fields according to $\alpha\bar{n} \ll \mu_{gen}V_j/d^2$, which automatically also satisfies $\beta n_0 \ll \mu_{gen}V_j/d^2$. Since $d^2/\mu_{gen}V_j$ is the transit time required for generated charges to drift the distance between the electrodes, this means that the field depletes the newly generated charges much faster than they are generated, such that the concentrations of newly generated micelles $n_{gen,+}$ and $n_{gen,-}$ in the bulk are much smaller than the equilibrium concentration $\bar{n}$. As a result the recombination term $-\alpha n_{tot,+}n_{tot,-}$ can be ignored in eqs 3 and 4. It also means that the generation of charges is so small that n_0 remains roughly equal to the equilibrium value $\bar{n}_0$, such that βn_0^2 can be replaced with $\alpha\bar{n}^2$ and the accumulation of newly generated charged inverse micelles at the electrodes is negligible compared to the amount of initially present charges on the time scales considered here.

Let us first consider the system in equilibrium in the absence of a field. If a voltage V_1 at $t = 0$ is applied starting from the homogeneous initial situation, we find with eq 5 that the electric field is $E_1 = V_1/d$ and the initial current with eq 1 is $I(0) = 2ze\bar{n}S\mu V_1/d$. The details of the full transient current related to the initially present charges depend on two parameters: $\varphi_1 = zeV_1/kT$ and $\lambda = 2z^2e^2d^2\bar{n}/\varepsilon_0\varepsilon_r kT$, but in all cases where $\varphi_1 \gg 1$ the initially present charged inverse micelles eventually get separated[27,28,30] corresponding to a total transported charge $Q = ze\bar{n}dS$. During this transient the concentration of newly generated inverse micelles gradually increases according to eq 3 until quasi steady-state is reached. In the quasi steady-state situation after the transient, the initially present charged inverse micelles have formed thin double layers at the electrodes with thickness approximately $2d/\varphi_1$ and they do not contribute any longer to the electric current. In the case that $\lambda < 20e^{\varphi_1/4}$, which is satisfied easily if $\varphi_1 \gg 1$, the effect of space-charge in the double layers on the electric field in the bulk is negligible since it is compensated mostly by image-charge in the electrodes.[27] For example, for $\varphi_1 = 394$ and $\lambda = 1.17 \times 10^5$, which corresponds respectively to a typical applied voltage of 10 V and the highest surfactant concentration used in our experiments, the voltage drop over the double layers in steady-state is only about 3% of the applied voltage. As will be confirmed later also the space-charge due to the generated charges in the bulk $ze(n_{gen,+} - n_{gen,-})$ is sufficiently low that its effect on the field can be ignored. Therefore, the field in the bulk is in good approximation $E_1 = V_1/d$. With the above assumptions (ignoring recombination and diffusion), eq 3 can be simplified such that the concentration profile of newly generated charged inverse micelles in the bulk in quasi steady-state is determined by

$$\pm\mu_{gen}E_1\frac{dn_{gen,\pm}}{dx} = \beta n_0^2 \tag{6}$$

Since no charges are generated at the electrodes, the flux of generated charged inverse micelles is zero at the electrodes of the same polarity, resulting in the boundary condition $\mu_{gen}E_1n_{gen,+}(x = 0) = \mu_{gen}E_1n_{gen,-}(x = d) = 0$. Due to the same blocking boundary condition, the newly generated charged inverse micelles accumulate at the oppositely polarized electrodes. However, because of the high applied voltage, these charges are forced into very thin regions at the electrodes where they are almost completely compensated by mirror charges in the electrodes, very similarly as for the initially present charges. As a result the generated charges accumulating at the electrodes have a negligible effect on the steady-state situation at voltage V_1 as well as on the transient current upon increasing the voltage from V_1 to V_2. In our analytical model we have approximated this situation by ignoring diffusion which even results in infinitely thin layers of accumulating charge at the electrodes and consequently full neutralization by mirror charges. Therefore, if we ignore these thin, electrically neutralized layers of charge at the attracting electrodes, the concentration profile of generated charges in the bulk can be described mathematically by not applying the blocking boundary condition at the attracting electrodes.[28] Then, eq 6 is also valid at the electrode of opposite polarity to the micelle charge. With these boundary conditions eq 6 results in linearly increasing and decreasing concentration profiles of positively and negatively charged newly generated inverse micelles: $n_{gen,+} = \beta n_0^2 dx/\mu_{gen}V_1$ and $n_{gen,-} = \beta n_0^2 d(1 - (x/d)/\mu_{gen}V_1$. As expected, the flux of generated charged inverse micelles is then zero at the electrode of the same polarity while the maximum flux is $\beta n_0^2 d$ at the oppositely polarized electrode. Then, the number of generated positively (or negatively) charged micelles in the bulk is $N_{gen,\pm} = (\beta n_0^2 d^3 S/2\mu_{gen}V_1)$, corresponding to an average concentration of $\langle n_{gen,\pm}\rangle = (\beta n_0^2 d^2/2\mu_{gen}V_1)$. The fact that the concentration of generated charges in the bulk scales inversely with voltage is counterintuitive. It can be understood from the fact that the generation rate is independent of the voltage. Therefore, a higher electric field does not generate more charges but in contrast depletes the charges faster and reduces their concentration. We can now re-evaluate the assumption of low space-charge in the bulk. From eq 5 it can be shown that by assuming $(ze\beta n_0^2 d^4/\varepsilon_0\varepsilon_r\mu_{gen}) \ll V_1^2$ the field in the bulk is not affected by the space-charge due to the generated charges, such that the assumption of a bulk field $E_1 = V_1/d$ is valid. The nonzero quasi steady-state current $I_{gen,lim}$ is obtained from eq 1:

$$I_{gen,lim} = \left(2ze\frac{\beta n_0^2 d^3 S}{2\mu_{gen}V_1}\right)\left(\frac{\mu_{gen}V_1}{d^2}\right) = \beta n_0^2 zedS \tag{7}$$

Equation 7 illustrates why $I_{gen,lim}$ does not depend on the applied voltage or the mobility μ_{gen} of the newly generated charged inverse micelles. The first factor between brackets $(2ze(\beta n_0^2 d^3 S/2\mu_{gen}V_1))$ is the total charge $2zeN_{gen,\pm}$ of generated charged inverse micelles in the bulk, which decreases with the speed $\mu_{gen}V_1/d$ of the micelles. The second factor $(\mu_{gen}V_1/d^2)$ however increases proportionally with this speed. This factor is the inverse of the transit-time for generated charged inverse micelles moving with speed $\mu_{gen}V_1/d$. Therefore, both μ_{gen} and V_1 disappear from the formula, and $I_{gen,lim}$ is called the "generation-limited" current. It is also called a "quasi steady-state" current since on a much longer time scale the bulk concentration of uncharged micelles will eventually decrease and the charge at the electrodes will increase by the continuous generation.

When, in the quasi steady-state situation at applied voltage V_1, the voltage is switched to a higher voltage $(V_1 \rightarrow V_2)$ at $t = 0$, the resulting current can be interpreted as the sum of two parts: the transient generation current $I_{gen,trans}(t)$ due to

DOI: 10.1021/jp511378k
J. Phys. Chem. B 2015, 119, 1957−1965

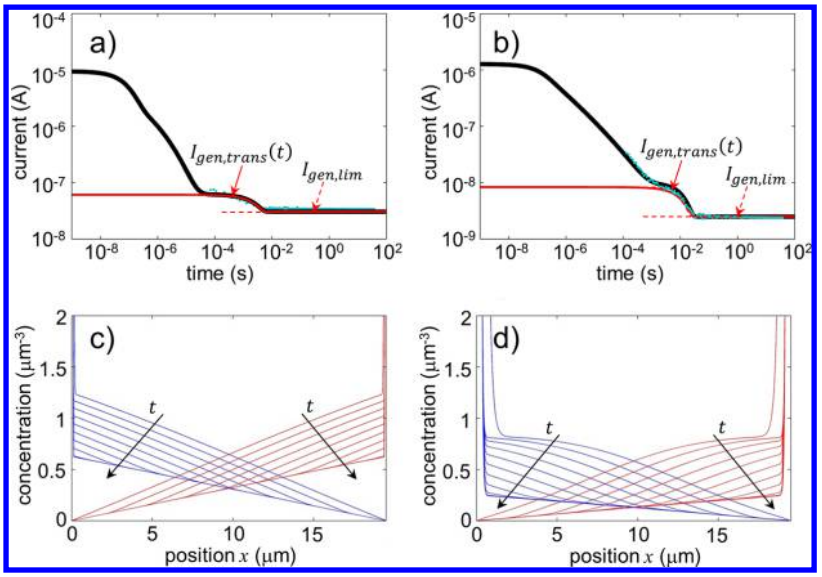

Figure 1. Simulation (black line), analytical model for the transient generation current (red line), level of the generation-limited current (dotted red line), and transient current measurement (blue dots) in (a) for $\overline{n}$ = 439 μm^{-3}, V_1 = 30 V, and V_2 = 60 V and in (b) for $\overline{n}$ = 70 μm^{-3}, V_1 = 3 V, and V_2 = 10 V. In (c–d), the corresponding concentration profiles of positive (red lines) and negative (blue lines) charges are shown at linearly spaced times during the transient.

generated charged inverse micelles and the double layer rearrangement current $I_{DL}(t)$ related to the initially present charged inverse micelles:

$$I_{V_1 \to V_2}(t) = I_{gen,trans}(t) + I_{DL}(t) \tag{8}$$

The transient generation current $I_{gen,trans}(t)$ has two contributions. One is related to the fixed amount of generated charged inverse micelles $N_{gen,\pm}$ already present at $t = 0$ which suddenly move faster due to the increased field, while another contribution results from newly generated charged inverse micelles. The concentration profile $n_{gen,\pm}$ related to the fixed amount of charge of the first contribution can be modeled according to eq 3 but without the generation and recombination term and ignoring diffusion:

$$\frac{dn_{gen,\pm}}{dt} = \mp \mu_{gen} E_2 \frac{dn_{gen,\pm}}{dx} \tag{9}$$

Here, the field in the bulk is given by $E_2 = V_2/d$. Using the steady-state concentration of generated charges in the bulk given by eq 6, we find that the gradient $(dn_{gen,\pm}/dx) = \mp(\beta n_0^2 d/\mu_{gen} V_1)$ at $t = 0$ is independent of the position. Therefore, eq 9 results in $(dn_{gen,\pm}/dt) = -(V_2/V_1)\beta n_0^2$, showing that the concentration at each position x decreases linearly in time at the same rate until it reaches the new equilibrium value $n_{gen,+} = \beta n_0^2\ dx/\mu_{gen} V_2$ and $n_{gen,-} = \beta n_0^2 d(1 - (x/d))/\mu_{gen} V_2$. Two regions are formed as time passes, one in which the new equilibrium is already reached, and one in which the gradient remains $(dn_{gen,\pm}/dx) = \mp(\beta n_0^2 d/\mu_{gen} V_1)$. The resulting concentration $n_{gen,+}(x, t)$ during the transient is given by

$$n_{gen,+} = \begin{cases} \dfrac{\beta n_0^2 d}{\mu_{gen} V_2} x,\ x \in \left[0,\ \dfrac{\mu_{gen} V_2 t}{d}\right] \\ \dfrac{\beta n_0^2 d}{\mu_{gen} V_1} x - \beta n_0^2 t\left(\dfrac{V_2}{V_1} - 1\right),\ x \in \left[\dfrac{\mu_{gen} V_2 t}{d},\ d\right] \end{cases} \tag{10}$$

where $n_{gen,-}(x) = n_{gen,+}(d - x, t)$. With eq 1 while ignoring diffusion by using $\Psi_i = En_i\mu_i$ the corresponding transient generation current becomes

$$I_{gen,trans}(t) = \begin{cases} \beta n_0^2 zedS\left\{\frac{V_2}{V_1} - \frac{2\mu_{gen} V_2 t}{d^2}\left(\frac{V_2}{V_1} - 1\right) + \frac{\mu_{gen}{}^2 V_2^2 t^2}{d^4}\left(\frac{V_2}{V_1} - 1\right)\right\},\ 0 \le t \le \frac{d^2}{\mu_{gen} V_2} \\ \beta n_0^2 zedS,\ \frac{d^2}{\mu_{gen} V_2} < t \end{cases} \tag{11}$$

The initial current $I_{gen,trans}(0) = V_2/V_1 \times I_{gen,lim}$ is again independent of the mobility of the generated micelles. But the transit time $t_{tr,2} = (d^2/\mu_{gen} V_2)$ for the generated micelles to reach the electrodes in the field V_2/d or for the current to return to the generation-limited value does depend on μ_{gen}. $I_{gen,trans}(t)$ is a quadratically decreasing current with time. Considering the derivative of the current at $t = 0$, initially the current appears to be linearly decreasing and would become zero at $t = (t_{tr,2}/2)(V_2/V_2 - V_1)$, but at this time the actual current is $I_{gen,trans}\ (t = (t_{tr,2}/2)(V_2/V_2 - V_1)) = I_{gen,trans}\ (t = 0) \times (V_2/4(V_2 - V_1)$. For values of $V_2/V_1 \gg 1$, this means that $I_{gen,trans}(t)$ first decreases in the time $t_{tr,2}/2$ to a quarter of the initial value, followed by a three times slower decrease until the current reaches steady-state at $t = t_{tr,2}$. After the transient the remaining quasi steady-state current $I_{gen,lim}$ causes an additional transported charge $\beta n_0^2 zedS\Delta t$ in each time interval Δt.

A charge moving between the electrodes causes a continuous current in the external circuit until it reaches the attracting electrode. The integral of the current is therefore a measure of the number of charges in the bulk and the amount of time they travel toward the electrodes. Equation 12 shows the integral of the transient generation current in eq 11 from $t = 0$ to $t = t_{tr,2}$, which corresponds to the charge transported from the bulk toward the electrodes in the transit time. This charge can be written as the sum of two contributions. The first part due to the initially present generated charges is inversely proportional to the voltage V_1, since the concentration of generated charged inverse micelles is reduced for increasing V_1. The second part is due to the generation of new charged inverse micelles, and this is inversely proportional to V_2.

DOI: 10.1021/jp511378k
J. Phys. Chem. B 2015, 119, 1957–1965

$$Q_{\mathrm{gen,trans}} = \frac{\beta n_0^2 zeSd^3}{3\mu_{\mathrm{gen}} V_1} + \frac{2\beta n_0^2 zeSd^3}{3\mu_{\mathrm{gen}} V_2} \tag{12}$$

For large values of V_2/V_1, $Q_{\mathrm{gen,trans}}$ becomes almost equal to $2zeN_{\mathrm{gen},\pm}/3$, such that the measurement of $Q_{\mathrm{gen,trans}}$ can be used to estimate $N_{\mathrm{gen},\pm}$. The mobility μ_{gen} can be estimated from the transit time $t_{\mathrm{tr},2} = (d^2/\mu_{\mathrm{gen}}V_2)$ or using $Q_{\mathrm{gen,trans}} \cong I_{\mathrm{gen,trans}}(0)\cdot(t_{\mathrm{tr},2}/3)$. The parabolic shape of the transient current is a direct result of the assumption of bulk generation, since in the steady-state this leads to a linearly increasing or decreasing concentrations of generated charges between the electrodes. In contrast, surface generation would lead to a uniform distribution of generated charged micelles, and to a linearly decreasing transient generation current with the same transit time $t_{\mathrm{tr},2} = (d^2/\mu_{\mathrm{gen}}V_2)$. Therefore, analysis of the measured transient generation current not only provides μ_{gen} and $N_{\mathrm{gen},\pm}$, it can also confirm bulk generation as the origin of the generation current.

The second part in eq 8, the double-layer current $I_{\mathrm{DL}}(t)$, is the result of the rearrangement of the double-layers of the initially present positively and negatively charged inverse micelles, both having a fixed total charge $\bar{n}dS$. In the steady-state at voltage V_1 the electric field is roughly $E \cong V_1/d$ in the bulk, but close to the electrodes the field increases strongly. Inside the thin double-layers at the electrodes the drift caused by the electric field is compensated by diffusion, such that these charges have a zero current contribution. When at $t = 0$ the voltage is increased to V_2 the charge $\bar{n}dS$ in both the positively and the negatively charged double layer experiences an additional field $E = (V_2 - V_1)/d$ which is not compensated by diffusion. The net particle flux in the double layers becomes $\Psi_{\pm} = \pm \mu n_{\pm} (V_2 - V_1/d)$ causing the concentration distributions to shift toward the attracting electrodes with speed $v = \mu (V_2 - V_1)/d$. The corresponding current at $t = 0$ is straightforward: $I_{DL} (0) = 2ze\bar{n}S\mu(V_2 - V_1/d)$. The current decreases rapidly at time scales $t < 2d^2/(\mu(V_2 - V_1)\varphi_1)$ which is roughly the time needed for the nonlinear part of the double layer to reach equilibrium. After that, the linear part of the double layer reaches the new equilibrium leading to an exponentially decreasing current with amplitude $8ze\bar{n}S\mu (\varphi_1/\lambda)(V_2 - V_1/d)$ and time constant $\tau = d^2/\varphi_1\varphi_2 D$ (see Supporting Information):

$$I_{\mathrm{DL,linear}}(t) \cong 8ze\bar{n}S\mu\frac{\varphi_1}{\lambda}\left(\frac{V_2 - V_1}{d}\right)e^{-t/\tau} \tag{13}$$

Figure 1 illustrates both the numerical simulation model and the analytical equations described above. In these simulations eqs 2−5 are solved with the appropriate boundary conditions and with parameters matching with some of the experiments (see Section 3). More precisely, Figures 1a and c correspond to measurements with mass fraction $\phi_m = 0.1$ of OLOA11K in dodecane, using simulation parameters $S = 10^{-4}$ m^2, $d = 19.5$ μm, $\varepsilon_r = 2$ and $T = 298$ K, $\bar{n} = 439$ μm^{-3}, $\mu = \mu_{\mathrm{gen}} = 1.00 \times 10^{-9}$ m^2 V^{-1} s^{-1}, $\alpha = 5.1 \times 10^{-22}$ m^3 s^{-1}, $V_1 = 30$ V, and $V_2 = 60$ V. Figures 1b and d correspond to measurements of $\phi_{\mathrm{m}} = 0.01$ with the same parameters except $\bar{n} = 70$ μm^{-3}, $\mu = \mu_{\mathrm{gen}} = 1.15 \times 10^{-9}$ m^2 V^{-1} s^{-1}, $\alpha = 2.05 \times 10^{-22}$ m^3 s^{-1}, $V_1 = 3$ V, and $V_2 = 10$ V. Using the value $(\alpha/\beta)^{1/2} \cong 51$ estimated from the very similar surfactant OLOA1200[29,35] corresponding values for β and $\bar{n}_0$ are obtained. Since $\beta \ll \alpha$ the generation rate is in good approximation $\beta\bar{n}_0^2 \cong \alpha\bar{n}^2$. In Figure 1a and b, the simulated electric current (black line) is shown, together with the analytical formula for the transient generation current in eq 11 (red line) and the level of the generation-limited current (dotted red line). Also measurements are shown corresponding to these parameters (blue dots) which are discussed in more detail in Section 3. The initial current $I_{V_1 \to V_2}(0)$ in the simulations matches well with the formula of the double layer current $I_{\mathrm{DL}}(0) = 2ze\bar{n}S\mu(V_2 - V_1/d)$. As explained earlier, the current decreases rapidly at time scales $t < 2d^2/(\mu(V_2 - V_1)\varphi_1)$ due to the nonlinear part of the double layer reaching its new equilibrium. This time scale corresponds to $t < 21$ μs in Figure 1a and $t < 0.9$ ms in Figure 1b. After that the double layer current decreases roughly exponentially due to the linear part of the double layer reaching equilibrium, matching well in amplitude and time-scale with the exponential decay given in eq 13. However, this exponential part of the double layer current cannot be observed in the total current because of the larger contribution from the transient generation current at $t >$ 40 μs in Figure 1a and $t > 1$ ms in Figure 1b. After that time the simulated current matches well with the analytical model of the transient generation current (eq 11). Figure 1c and d give the concentrations of positive charges (red) and negative charges (blue) at times $t = j \times d^2/8\mu V_2$ with $j = 0, 1, ..., 10$. The linearly decreasing concentration profile with time given by eq 10 is illustrated in Figure 1c. When the voltage V_1 is not sufficiently high, the space-charge due to the generated charged inverse micelles can lead to a steady-state bulk field that is lower than $E \cong V_1/d$ and spatially inhomogeneous.[30] As a result of $E < V_1/d$, the concentration of generated charges in steady-state can be higher than expected from eq 10 and nonlinearly increasing. This case is illustrated in Figure 1d, where the curve for $t = 0$ corresponds to the steady-state distribution at voltage V_1. As a result the simulated transient generation current shown in Figure 1b is slightly higher than predicted by the model.

3. TRANSIENT CURRENT EXPERIMENTS

3.1. Materials and Methods. Solutions are prepared with mass fractions $\phi_{\mathrm{m}} = 0.01$, 0.03, and 0.1 of OLOA11K (Chevron Oronite) in *n*-dodecane (Rectapur, VWR). The solutions are inserted in a device with plane parallel, plain ITO electrodes with overlapping area $S = 10^{-4}$ m^2. The two electrodes are separated at fixed at a certain distance using UV-curing glue (Norland Optics) containing spacer beads. The distance $d = 19.5$ μm is measured with interferometry (PerkinElmer Lambda 950). The current measurements are performed using a custom-built setup consisting of a Keithley 428 current amplifier and a National Instruments USB-6212 data acquisition module for the synchronized generation of voltages and the sampling of the electric current. The cell is placed inside a closed metallic box to screen it from external electric fields and is measured at room temperature. To obtain homogeneous initial conditions, the electrodes are short-circuited for 500 s before each measurement. Currents measured for pure dodecane ($\phi_{\mathrm{m}} = 0$) are roughly 500 times lower than those for the lowest surfactant concentration used here and are limited by the sensitivity of the experimental setup. This corresponds to a bulk conductivity of dodecane below 10^{-13} Ω^{-1} m^{-1}, indicating that the used dodecane does not contain much charge contaminants.

3.2. Measurements. Transient currents have been measured for the different concentrations of OLOA11K and for different applied voltage steps across the electrodes: 0 V → V_1 (polarizing current) and $V_1 \to V_2$ (transient generation

DOI: 10.1021/jp511378k
J. Phys. Chem. B 2015, 119, 1957−1965

current). The polarizing voltages are applied for 40 s, which is sufficient to completely separate the initially present charges. Figure 2 shows the results for the currents for $V_1 \rightarrow V_2$, in (a)

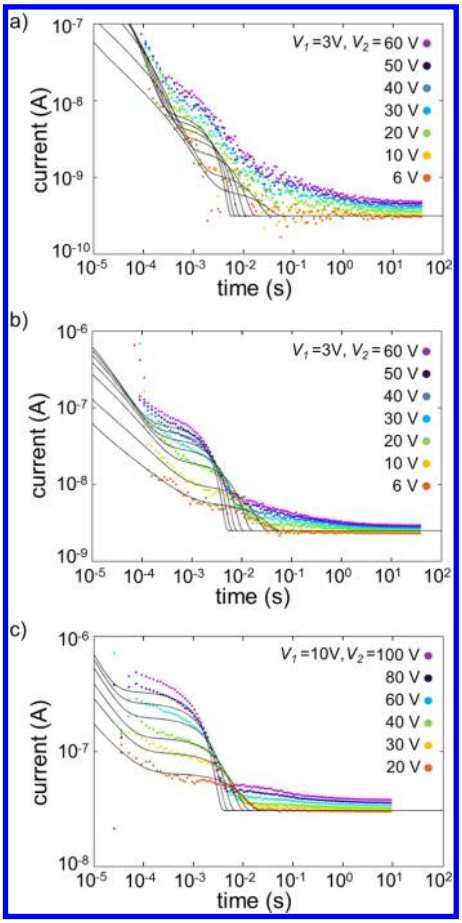

Figure 2. Measurements (colored dots) and simulations (black lines) of transient currents for $V_1 \rightarrow V_2$, for ϕ_m = 0.01 (a), 0.03 (b), and 0.1 (c).

for ϕ_m =0.01 and in (b) for ϕ_m = 0.03, both with V_1 = 3 V and V_2 = 6, 10, 20, 30, 40, 50, and 60 V, and in (c) for ϕ_m = 0.1 with V_1 = 10 V and V_2 = 20, 30, 40, 60, 80, and 100 V. For each experiment four measurement runs are averaged.

3.3. Analysis. Using the theory from Section 2, we can now analyze the transient currents in more detail. From the polarizing currents (0 V $\rightarrow$ V_1) (not shown) the equilibrium concentration of initially present charged inverse micelles can be estimated as $\bar{n} = \int_0^{t_{tr}} (I(t) - I_{SS})\, dt/zedS$, where I_{SS} is the small quasi steady-state current obtained at t = 10 s and t_{tr} is the transit time at which all initially present charges have arrived at the electrodes. Figure 3 shows that the obtained concentrations $\bar{n}$ = 70, 165, and 439 μm^{-3}, respectively, for ϕ_m = 0.01, 0.03, and 0.1 follow roughly the linear relation $\bar{n} \cong 4500\ \mu m^{-3} \times \phi_m$ (red trendline) which is in good agreement with values for OLOA1200.[27,31,34] As explained in Section 2, from the law of mass action for disproportionation it is expected that in equilibrium and in the absence of a field $\bar{n}^2/n_0^2$ is constant such that $\bar{n}$ is proportional to n_0. If we assume that the concentration of inverse micelles scales proportionally to the surfactant concentration, this leads to a proportionality between $\bar{n}$ and ϕ_m. Therefore, the observed proportionality between $\bar{n}$ and ϕ_m

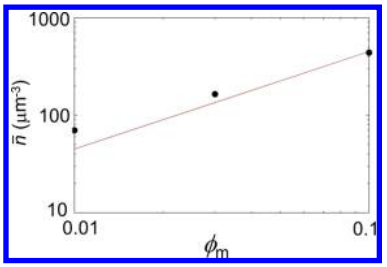

Figure 3. Equilibrium concentration of charged inverse micelles $\bar{n}$ increases linearly with the surfactant mass fraction, as shown by the linear trendline (red line) $\bar{n} \cong 4500\ \mu m^{-3} \times \phi_m$.

validates the assumption of a disproportionation generation mechanism.

The mobility of the initially present charges is obtained as $\mu = I(0)d/2ze\bar{n}SV_1$. The diffusion coefficient $D = \mu kT/ze$ is used to obtain the hydrodynamic radius of the charged inverse micelles $r_\pm = kT/6\pi\eta D$ with the viscosity of dodecane $\eta = 1.38 \times 10^{-3}$ Pa·s. For the mobilities we find $\mu = 1.15 \times 10^{-9}$ m^2 V^{-1} s^{-1}, 1.25×10^{-9} m^2 V^{-1} s^{-1}, and 1.00×10^{-9} m^2 V^{-1} s^{-1}, respectively, for ϕ_m = 0.01, 0.03, and 0.1, so $\mu \cong (1.1 \pm 0.1) \times 10^{-9}$ m^2 V^{-1} s^{-1}, $D \cong (2.9 \pm 0.2) \times 10^{-11}$ m^2 s^{-1} and $r_\pm = (5.5 \pm 0.7)$ nm. This size of the inverse micelles is consistent with previous studies with transient current measurements showing a radius of about 6–7 nm.[22,27,31]

In Figure 2, it can be observed that the quasi-steady-state current increases slightly (less than a factor 1.5) when the voltage increases a factor of 10 (from 6 to 60 V) or a factor of 5 (from 20 to 100 V), which is not expected in our model of bulk disproportionation leading to a voltage-independent, generation-limited current. The observed increase in current can be attributed to small additional effects such as surface generation which will be ignored in our analysis. Figure 4 shows the

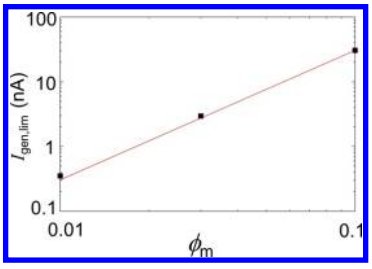

Figure 4. Generation-limited quasi steady-state current scales quadratically with the surfactant mass fraction for ϕ_m = 0.01, 0.03, and 0.1. The trendline (red line) shows $I_{gen,lim} = 3.05 \times 10^{-6}$ A $\times \phi_m^2$.

generation-limited currents $I_{gen,lim} = 3.14 \times 10^{-10}$ A, 2.5×10^{-9} A, and 3.05×10^{-8} A, respectively, for ϕ_m = 0.01, 0.03, and 0.1, obtained at 6 V for ϕ_m = 0.01 and 0.03 and at 20 V for ϕ_m = 0.1. Using $I_{gen,lim} = \beta n_0^2 zedS$ from eq 7, this allows us to obtain $\beta n_0^2 \cong \beta \bar{n}_0^2 = \alpha \bar{n}^2$. Then, since $\bar{n}$ is known a value for the recombination rate constant α can be found. As explained before, β and $\bar{n}_0$ are obtained using the value $(\alpha/\beta)^{1/2} \cong 51$ from an estimation of the concentration of uncharged inverse micelles in OLOA1200.[29,35] Considering the linear relationship between $\bar{n}$ and ϕ_m (see Figure 3) the trendline $I_{gen,lim} = 3.05 \times 10^{-6}$ A $\times \phi_m^2$ shows that $I_{gen,lim}$ is in fact proportional to $\bar{n}^2$, which is expected for a disproportionation model. The average value of the recombination constant is $\alpha = 3.4 \times 10^{-22}$ m^3 s^{-1}.

Using the analytical model and simulations, we can now extract the concentration and mobility of newly generated

DOI: 10.1021/jp511378k
J. Phys. Chem. B 2015, 119, 1957–1965

charged inverse micelles from the transient generation currents in Figure 2a–c. An estimation of $Q_{gen,trans}$ can be made by integrating the current while correcting for the exponential part of the double layer current and the quasi steady-state current. In a first example of the measurement in Figure 2b with ϕ_m = 0.03, V_1 = 3 V, and V_2 = 60 V, we find $Q_{gen,trans}$ = 1.51 × 10^{-10} C. Then, under the assumption that $Q_{gen,trans} \cong 2zeN_{gen,\pm}/3$, which is valid for large values of V_2/V_1, the value $N_{gen,\pm}$ = 1.41 × 10^9 is obtained for the amount of generated charged inverse micelles present in the bulk in steady state at voltage V_1 = 3 V. This corresponds to an average concentration of $\langle n_{gen,\pm} \rangle$ = 0.72 μm^{-3}, which is 230 times lower than the equilibrium concentration $\overline{n}$ = 165 μm^{-3}. The transit time $t_{tr,2}$ = 5.1 ms can be used to estimate the mobility of the newly generated charged inverse micelles $\mu_{gen} = d^2/t_{tr,2}V_2$ = 1.24 × 10^{-9} m^2 V^{-1} s^{-1}. This mobility corresponds well with the value μ = 1.25× 10^{-9} m^2 V^{-1} s^{-1} of the initially present charged inverse micelles obtained for ϕ_m = 0.03. In a second example of the measurement in Figure 2c with ϕ_m = 0.1, V_1 = 10 V, and V_2 = 60 V, we find $Q_{gen,trans}$ = 4.16 × 10^{-10} C with corresponding values $N_{gen,\pm}$ = 3.90 × 10^9, $\langle n_{gen,\pm} \rangle$ = 2.00 μm^{-3} (220 times lower than the equilibrium concentration $\overline{n}$ = 439 μm^{-3}). The transit time $t_{tr,2}$ = 5.3 ms results in μ_{gen} = 1.20 × 10^{-9} m^2 V^{-1} s^{-1}, which is comparable to the value μ = 1.00 × 10^{-9} m^2 V^{-1} s^{-1} of the initially present charged inverse micelles obtained for ϕ_m = 0.1.

A good agreement is obtained between the simulations and the experiments of Figure 2 taking values of μ_{gen} that are equal to μ. Therefore, we can assume that the size of newly generated inverse micelles is about the same as the size of the initially present charged inverse micelles. The simulations in Figure 2 are carried out with parameters S = 10^{-4} m^2, d = 19.5 μm, ε_r = 2, and T = 298 K and in (a) for $\overline{n}$ = 70 μm^{-3}, $\mu = \mu_{gen}$ = 1.15 × 10^{-9} m^2 V^{-1} s^{-1}, α = 2.05 × 10^{-22} m^3 s^{-1}, in (b) for $\overline{n}$ = 165 μm^{-3}, $\mu = \mu_{gen}$ = 1.25 × 10^{-9} $m^2V^{-1}s^{-1}$, α = 2.94 × 10^{-22} m^3s^{-1}, both with V_1 = 3 Vm and V_2 = 6, 10, 20, 30, 40, 50, and 60 V, and in (c) for $\overline{n}$ = 439 μm^{-3}, $\mu = \mu_{gen}$ = 1.00 × 10^{-9} m^2 V^{-1} s^{-1}, α = 5.1 × 10^{-22} m^3 s^{-1} for V_1 = 10 V, and V_2 = 20, 30, 40, 60, 80, and 100 V.

Figure 5 shows data from Figure 2c on a linear scale, illustrating that the transient generation current can indeed be

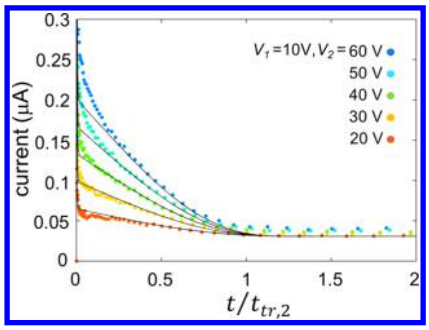

Figure 5. Measurements and simulations (black lines) of the transient generation current for ϕ_m = 0.1 and V_1 = 10 V and V_2 = 20–60 V in steps of 10 V from Figure 2c but on linear and normalized axes.

described well by the quadratically decreasing current in eq 11. For better visibility, the time axis has been normalized to the transit-time $t_{tr,2}$ = $(d^2/\mu_{gen}V_2)$, using fixed values d = 19.5 μm and μ_{gen} = 1.15 × 10^{-9} m^2 V^{-1} s^{-1}. This provides direct evidence for a bulk generation mechanism. For comparison, if surface generation was the mechanism generating the charges, there would be a homogeneous concentration of charges in steady state, and the transient generation current would be linearly decreasing. Fitting a linearly decreasing current to the experimental data would result in two times higher values of the mobility as for the case of bulk generation. However, surface generation is in contradiction with the observation that the generation-limited current is proportional to d (for OLOA1200[27,34]), which indicates that the generation is occurring in the bulk. While there is a good match between measurement and simulation for V_2 < 30 V in Figure 2b and c, it should be noted that for V_2 > 30 V an additional linearly decreasing current appears corresponding to charges with a higher mobility. The fact that this effect is absent for low values of V_2 but becomes more important for higher voltages V_2 suggests that these faster charges are released from the electrodes when increasing the voltage to V_2 rather than that they are already present in the bulk in steady-state.

Since the part of the double layer current before t = 10^{-4} s cannot be measured with our setup, Q_{DL} cannot be estimated. Only between t = 10^{-4} s and t = 10^{-3} s in the different measurements of Figure 2, the good agreement in both amplitude and time-scale can be observed between measurements and simulations of the double layer current. This confirms that in steady-state the initially present charged inverse micelles form a diffuse double layer as expected from the Nernst–Planck–Poisson equations.

4. DISCUSSION

The described transient generation current method is applicable with some restrictions. The generation rate of the surfactant system should be sufficiently low and the voltage V_1 high enough such that the generation-limited steady-state current can be measured. But V_2/V_1 should also be large enough to get a sufficiently high amplitude of the transient generation current. However, the higher V_2, the faster this transient occurs, and the more difficult it becomes to measure. Since the generation-limited current scales quadratically with ϕ_m, for $\phi_m \ll 0.01$ the generation-limited current becomes so low that the measurement sensitivity and other current generation effects start playing a role. For that reason it is difficult to draw conclusions from the data from Figure 1a other than that the time-constants and amplitudes are roughly as expected. For concentrations 0.01 < $\phi_m \leq$ 0.1, the signal-to-noise ratio is good. For high concentrations ($\phi_m \gg 0.1$), the generation rate increases, and higher voltages are required to measure the generation-limited current. Also, the presented theory and analytical model should be modified depending on the electrical behavior of the surfactant solution. For example, for AOT in dodecane the double layer current will be absent since the charged AOT inverse micelles do not form a classical double layer.[17,32,33]

The presented results confirm in more detail the established theory that bulk disproportionation is the dominant generation mechanism at typical surfactant concentrations. However, the knowledge that a similar hydrodynamic size is obtained for both the newly generated and the initially present charged inverse micelles is an important step toward understanding the differences which have been observed between both types of micelles.

DOI: 10.1021/jp511378k
J. Phys. Chem. B 2015, 119, 1957–1965

5. CONCLUSION

In conclusion, the analysis of transient generation currents with stepwise increasing voltages has been used to investigate the generation mechanism of charged inverse micelles of the surfactant OLOA11K in dodecane. Simulations and analytical approximations based on bulk disproportionation have been developed to analyze the current measurements. It is found that the size of the newly generated charged inverse micelles is roughly the same as the size of the charged inverse micelles present in equilibrium, which is important in understanding observed differences between both types of micelles. A detailed current analysis confirms that the charges are generated in the bulk and according to a disproportionation mechanism.

■ ASSOCIATED CONTENT

Ⓢ Supporting Information

Analytical model for the double layer current. This material is available free of charge via the Internet at http://pubs.acs.org.

■ AUTHOR INFORMATION

Corresponding Author

*E-mail: filip.strubbe@elis.ugent.be.

Notes

The authors declare no competing financial interest.

■ ACKNOWLEDGMENTS

This research was supported by the Research Foundation—Flanders (FWO Vlaanderen), IWT-Vlaanderen, the IAP project photon@be funded by the Belgian Science Policy program, and the Hercules Foundation.

■ REFERENCES

(1) Fowkes, F. M.; Pugh, R. J. The Dispersibility and Stability of Coal Particles in Hydrocarbon Media with a Polyisobutene Succinamide Dispersing Agent. *Colloids Surf.* **1984**, *11*, 423−427.

(2) Won, Y.-Y.; Meeker, S. P.; Trappe, V.; Weitz, D. A.; Diggs, N. Z.; Emert, J. I. Effect of Temperature on Carbon-Black Agglomeration in Hydrocarbon Liquid with Adsorbed Dispersant. *Langmuir* **2005**, *21*, 924−932.

(3) Walmsley, H. L. The Avoidance of Electrostatic Hazards in the Petroleum Industry. *J. Electrostat.* **1992**, *27*, 1−193.

(4) Sierota, A.; Rungis, J. Electrostatic Charging in Transformer Oils. *IEEE Trans. Dielect. Elect. Insulation* **1994**, *1*, 840−870.

(5) Comiskey, B.; Albert, J. D.; Yoshizawa, H.; Jacobson, J. An Electrophoretic Ink for All-Printed Reflective Electronic Displays. *Nature* **1998**, *394*, 253−255.

(6) Verschueren, A. R. M.; Stofmeel, L. W. G.; Baesjou, P. J.; van Delden, M. H. W. M.; van Glabbeek, J. J.; Lenssen, K.-M. H.; Mueller, M.; Osenga, J. T. M.; Oversluizen, G.; Schuurbiers, R. M. Optical Performance of In-Plane Electrophoretic Color E-Paper. *J. Soc. Inf. Dispersion* **2010**, *18*, 1−7.

(7) Kim, J. Y.; Garoff, S.; Anderson, J. L.; Schlangen, L. J. M. Movement of Colloidal Particles in Two-Dimensional Electric Fields. *Langmuir* **2005**, *21*, 10941−10947.

(8) Morrison, I. D. Electrical Charges in Nonaqueous Media. *Colloids Surf., A* **1993**, *71*, 1−37.

(9) Smith, G. N.; Eastoe, J. Controlling Colloid Charge in Nonpolar Liquids with Surfactants. *Phys. Chem. Chem. Phys.* **2013**, *15*, 424−439.

(10) Roberts, G. S.; Sanchez, R.; Kemp, R.; Wood, T.; Bartlett, P. Electrostatic Charging of Nonpolar Colloids by Reverse Micelles. *Langmuir* **2008**, *24*, 6530−6541.

(11) Hsu, M. F.; Dufresne, E. R.; Weitz, D. A. Charge Stabilization in Nonpolar Solvents. *Langmuir* **2005**, *21*, 4881−4887.

(12) Dukhin, A. S.; Goetz, P. J. How Non-Ionic "Electrically Neutral" Surfactants Enhance Electrical Conductivity and Ion Stability in Non-Polar Liquids. *J. Electroanal. Chem.* **2006**, *588*, 44−50.

(13) Lyklema, J. Principles of Interactions in Non-Aqueous Electrolyte Solutions. *Curr. Opin. Colloid Interfaces* **2013**, *18*, 116−128.

(14) Dukhin, A.; Parlia, S. Ions, Ion Pairs and Inverse Micelles in Non-Polar Media. *Curr. Opin. Colloid Interfaces* **2013**, *18*, 93−115.

(15) Strubbe, F.; Beunis, F.; Marescaux, M.; Verboven, B.; Neyts, K. Electrokinetics of Colloidal Particles in Nonpolar Media Containing Charged Inverse Micelles. *Appl. Phys. Lett.* **2008**, *93*, 254106.

(16) Strubbe, F.; Beunis, F.; Brans, T.; Karvar, M.; Woestenborghs, W.; Neyts, K. Electrophoretic Retardation of Colloidal Particles in Nonpolar Liquids. *Phys. Rev. X* **2013**, *3*, 021001.

(17) Lin, T.; Kodger, T. E.; Weitz, D. A. Transport of Charged Colloids in a Nonpolar Solvent. *Soft Matter* **2013**, *9*, 5173−5177.

(18) Stotz, S. Field Dependence of the Electrophoretic Mobility of Particles Suspended in Low-Conductivity Liquids. *J. Colloid Interface Sci.* **1978**, *65*, 118−130.

(19) Sainis, S. K.; Merrill, J. W.; Dufresne, E. R. Electrostatic Interactions of Colloidal Particles at Vanishing Ionic Strength. *Langmuir* **2008**, *24*, 13334−13347.

(20) Beunis, F.; Strubbe, F.; Neyts, K.; Petrov, D. Beyond Millikan: The Dynamics of Charging Events on Individual Colloidal Particles. *Phys. Rev. Lett.* **2012**, *108*, 016101.

(21) Strubbe, F.; Beunis, F.; Neyts, K. Detection of Elementary Charges on Colloidal Particles. *Phys. Rev. Lett.* **2008**, *100*, 218301.

(22) Behrens, S. H.; Grier, D. G. Pair Interaction of Charged Colloidal Spheres near a Charged Wall. *Phys. Rev. E* **2001**, *64*, 050401.

(23) Guo, Q.; Singh, V.; Behrens, S. H. Electric Charging in Non-Polar Liquids Because of Nonionizable Surfactants. *Langmuir* **2010**, *26*, 3203−3207.

(24) Espinosa, C. E.; Guo, Q.; Singh, V.; Behrens, S. H. Particle Charging and Charge Screening in Nonpolar Dispersions with Non-Ionic Surfactants. *Langmuir* **2010**, *26*, 16941−16948.

(25) Novotny, V. Electrical Conduction in Surfactant-Water-Nonaqueous Liquid Systems. *J. Electrochem. Soc.* **1986**, *133*, 1629−1636.

(26) Cirillo, M.; Strubbe, F.; Neyts, K.; Hens, Z. Thermal Charging of Colloidal Quantum Dots in Apolar Solvents: A Current Transient Analysis. *ACS Nano* **2011**, *5*, 1345−1352.

(27) Verschueren, A. R. M.; Notten, P. H. L.; Schlangen, L. J. M.; Strubbe, F.; Beunis, F.; Neyts, K. Screening and Separation of Charges in Microscale Devices: Complete Planar Solution of the Poisson-Boltzmann Equation. *J. Phys. Chem. B* **2008**, *112*, 13038−13050.

(28) Beunis, F.; Strubbe, F.; Marescaux, M.; Beeckman, J.; Neyts, K.; Verschueren, A. R. M. Dynamics of Charge Transport in Planar Devices. *Phys. Rev. E* **2008**, *78*, 011502.

(29) Beunis, F.; Strubbe, F.; Karvar, M.; Drobchak, O.; Brans, T.; Neyts, K. Inverse Micelles as Charge Carriers in Nonpolar Liquids: Characterization with Current Measurements. *Curr. Opin. Colloid Interfaces* **2013**, *18*, 129−136.

(30) Neyts, K.; Karvar, M.; Drobchak, O.; Brans, T.; Strubbe, F.; Beunis, F. Simulation of Charge Transport and Steady State in Non-Polar Media Between Planar Electrodes with Insulating Layers. *Colloids Surf., A* **2014**, *440*, 101−109.

(31) Kornilovitch, P.; Jeon, Y. Transient Electrophoretic Current in a Nonpolar Solvent. *J. Appl. Phys.* **2011**, *109*, 064509.

(32) Karvar, M.; Strubbe, F.; Beunis, F.; Kemp, R.; Smith, A.; Goulding, M.; Neyts, K. Transport of Charged Aerosol OT Inverse Micelles in Nonpolar Liquids. *Langmuir* **2011**, *27*, 10386−10391.

(33) Karvar, M.; Strubbe, F.; Beunis, F.; Kemp, R.; Smith, N.; Goulding, M.; Neyts, K. Investigation of Various Types of Inverse Micelles in Nonpolar Liquids Using Transient Current Measurements. *Langmuir* **2014**, *30*, 12138−12143.

(34) Strubbe, F.; Verschueren, A. R. M.; Schlangen, L. J. M.; Beunis, F.; Neyts, K. Generation Current of Charged Micelles in Nonaqueous Liquids: Measurement and Simulations. *J. Colloid Interface Sci.* **2006**, *300*, 396−403.

DOI: 10.1021/jp511378k
J. Phys. Chem. B 2015, 119, 1957−1965

(35) Beunis, F.; Strubbe, F.; Marescaux, M.; Neyts, K.; Verschueren, A. R. M. Micellization and Adsorption of Surfactant in a Nonpolar Liquid in Micrometer Scale Geometries. *Appl. Phys. Lett.* **2010**, *97*, 181912.
(36) Prieve, D. C.; Hoggard, J. D.; Fu, R.; Sides, P. J.; Bethea, R. Two Independent Measurements of Debye Lengths in Doped Nonpolar Liquids. *Langmuir* **2008**, *24*, 1120−1132.

DOI: 10.1021/jp511378k
J. Phys. Chem. B 2015, 119, 1957−1965